STUDY OF NEWTONIAN FLUID DROPS RISING IN WATER

by J. MERCIER and W. ANCIÃES

Group of Engineering Sciences
Pontifícia Universidade Católica do Rio de Janeiro
209 Rua Marquês de São Vicante
Rio de Janeiro, Brazil

Introduction

The present work extends the study of deformable particles moving in liquids by investigating Newtonian fluid [1, 2] drops rising in water. Main topics treated for bubbles rising and drops falling in liquids are examined in this case.

Experimental works on bubbles rising [3, 4, 5] and drops falling [6, 7] in liquids have determined the variation of their velocity and drag coefficient vs. equivalent diameter D and Reynolds number respectively. Theoretical studies for bubbles [8, 9, 10, 11] and drops [8, 12, 13, 14] yield to those results within certain limited ranges. The shape of the bubbles [3, 4, 5] was found to vary successively from spherical ($D < 0.05$ cm) to ellipsoidal ($0.05 < D < 0.3$ cm) up to spherical cap ($D > 1.0$ cm). These cases have also been studied theoretically by [8, 9, 10, 11]. A constant drag coefficient has been found for spherical cap [4]. Shapes of drops falling in liquids also vary similarly in different ranges [6, 7, 15]. Pulsations were observed for both, spherical and ellipsoidal bubbles [3] and drops [16, 17, 18]. The trajectory followed by bubbles [3] and drops [6, 7, 16], in steady regime, was found experimentally to be : straight for small, zig-zag or circular helicoidal for medium and again straight-vertical for large ones. Trajectories have also been studied theoretically [3], under simplified assumptions.

The present paper is concerned with the behavior of Newtonian fluid drops of density less than one, rising in purified water. In the experimental part, photographic equipment has been set up to take plates giving a three-dimensional description of the motion of rising drops. A pair of sequence exposures (taken simultaneously in perpendicular focusing planes) has been used to obtain the kinematics of each rising drop studied. The constant vertical velocity component U, and the distance covered after release to reach it, were found to be a fixed property of the system. The corresponding drag coefficient has also been calculated. These results are shown on graphs vs. equivalent diameter and Reynolds numbers varying from 0.25 to 1.0 cm and 1 to 1,500 respectively. They are also expressed by empirical formulae and compared to the cases of rising bubbles and falling drops. Pulsations and shapes are described.

It is also shown that the trajectory of the drops, having a constant vertical velocity component U, follows a path approximated by what can be called an exponential helix. The path of drops (before being vertical) rising with constant velocity component was found to be not only a fixed property of the system but also to depend on the mode of release.

Experimental

The experimental part of the present work consisted of taking photographs, in a dark room, of drops rising in a container filled with purified water (Fig. 1). The experiments were carried out at constant temperature of 20 °C.

The square section of the prismatic container ($32 \times 32 \times 100$ cm) was sufficient, according to [16, 19], to

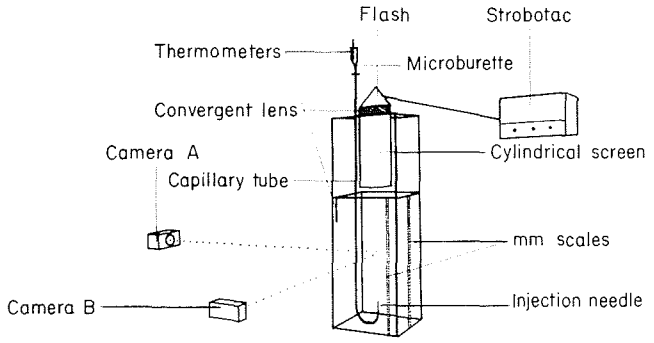

1/

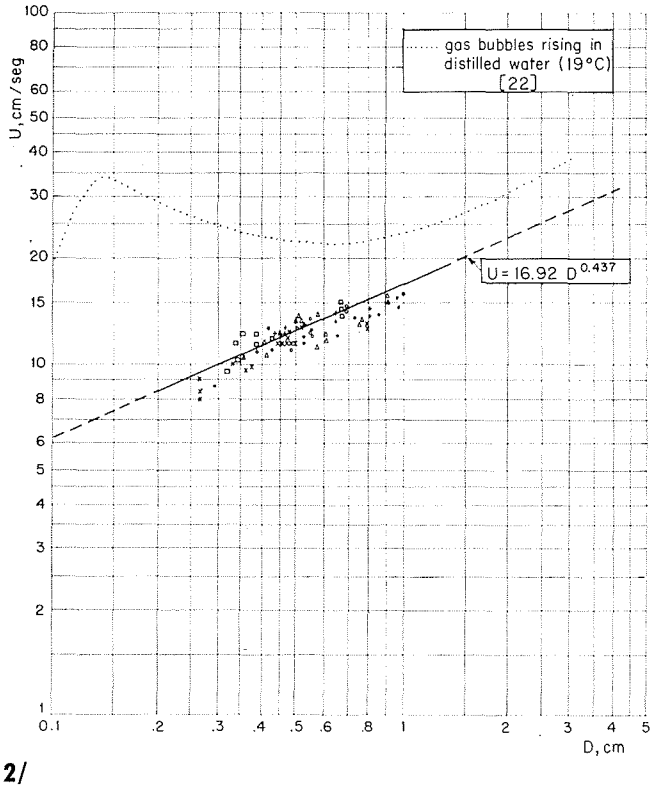

2/

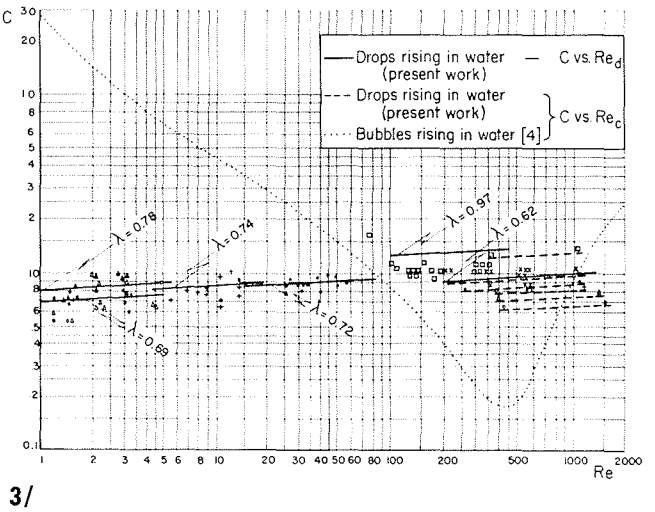

3/

1/ Experimental set-up (perspective).
Vue en perspective de l'installation expérimentale.

2/ Constant vertical component of velocity U vs equivalent diameter D.
La composante verticale constante U de la vitesse en fonction du diamètre équivalent D.

3/ Drag coefficient C vs. Reynolds numbers Re_c and Re_d.
Coefficient de traînée C en fonction des nombres de Reynolds Re_c et Re_d.

Table 1

Fluid properties at 20 °C

Phase	Fluid	Experimental results	ρ (g/cm³)	μ (cP)	λ
Continuous	Purified Water		1.05	1.00	
Discontinuous	Kerosene	□	0.80	2.50	0.97
Discontinuous	Xylene	×	0.85	0.85	0.62
Discontinuous	MVI- 40 Shell	●	0.86	15.50	0.72
Discontinuous	HVI- 65 Shell	+	0.87	70.00	0.74
Discontinuous	HVI-160 Shell	Δ	0.88	280.00	0.78
Discontinuous	MVI-170 Shell	O	0.90	420.00	0.69

avoid vertical wall effects on the drops. The walls were made of 0.5 cm thick crystal. The 6 Newtonian fluids described in Table 1 were used as dropping liquids. They were selected for reasons of density-difference, immiscibility with continuous phase and to cover ranges varying from 1 to 1,300 and 0.25 to 1.0 cm, for the Reynolds number Re_d and the equivalent diameter D respectively. Drops were formed and released by 14 combinations of injection needles (located in the center of the container's bottom) coupled to capillary tubes. The latter were connected to a micro burette Assistent 2 ml (with divisions of 0.01 ml), placed above the container. It was used to measure the volume of the drops and control their formation and release. Dynamical effects and perturbations due to the previous drop could thus be made negligeable. A variation of 1.5 % only was observed for each one of the 14 different volumes formed with each fluid. When changing discontinuous phases, purified water was substituted and all the equipment was throughly cleaned.

In order to record the trajectory of the drop exactly, two Leica-M2 cameras were placed in perpendicular vertical planes, intersecting on the releasing needle (Fig. 1). Parallax-free photographs were taken by those cameras with the power lenses left open at 400 cm away from the objective. Each pair of sequence exposures showing the rise of a drop was taken on stationary films (Kodak Tri X 135-36 negative film, ASA 400) using an intermittent flash (light persistent 3×10^{-4} s) controlled by a Brüel and Kjoer Strobotac. For each fluid, four pairs of plates were taken for each one of the 14 drop's volume. To follow the motion closely, though avoiding super exposure, flashing times of 0.1 and 0.05 s were used for each drop's volume. The flash was located above the container. A convergent lens and a 50 cm long cylindrical screen were placed below it to focus illumination on the drop's trajectory. Even so, only 30 cm of the trajectory covered with velocity U appears neatly on the plates because of light dispersion. Photographs of drops were related to their actual dimensions by two millimeter scales set in the camera fields.

Kinematics and dynamics of rising drops

The 4×14 (volumes) $\times$ 6 (discontinuous phases) photographs described above, were magnified to twice their actual size to describe and accurately calculate the following.

After release, the drops studied cover a distance of approximately twenty times their diameters D, before having a constant vertical velocity component U. During that initial unsteady rise, pulsations were observed for drops having a diameter D larger than 0.6 cm. The frequency was of the order of $2\ s^{-1}$ and the amplitude of 0.2 D. These pulsations were abruptly damped and disappeared completely when the drops reached constant U. For inverse cases of drop fall a frequency of the order of $10\ s^{-1}$ was observed in steady regime [20], corresponding to Lamb's formula [21]. The influence of the direction of motion on the pulsation of drops was thus shown to be predominant.

The constant velocity component U, and the distance covered after release to reach it, were found to be a fixed property of the system. As for bubbles (the density of the discontinuous phases varying little, see Table 1), the diameter D was the best parameter found to describe the variation of the drops velocity. Thus, the constant vertical velocity component of rising drops U was plotted vs. the equivalent diameter D, on Figure 2 using logarithmic scales. The above plot, showing little dispersion, was fairly well represented by a straight line the equation of which is :

$$U = 16.92\, D^{0.437} \qquad (1)$$

The variation of the velocity of rise of bubbles vs. diameter obtained in [22] is also shown on Figure 2 for comparison. The main difference between the U-curves of rising drops and bubbles is that the former, besides being obviously lower, does not show a minimum as the latter does (for the range of diameter studied, $0.25 < D < 1.0$ cm). Since Frounde's Number $F_r = U/\sqrt{(gD)}$ varies very little with the equivalent diameter D, formula (1) may also be conveniently written as :

$$U = 2.14\, (F_r)^{0.287}$$

In the variable used above, the Drag coefficient C is given by :

$$C = \frac{4}{3\,(F_r)^2}\left(\frac{\rho_c}{\rho_d} - 1\right) \qquad (2)$$

for rising drops [6, 9]. As for bubbles, the Reynolds number was the best parameter found to describe the variation of the drag coefficient. By substituting in (2) values taken from Table 1 and Figure 2, the drag coefficient C was then calculated and plotted in Figure 3 vs. the Reynolds numbers Re_d and Re_c, varying from 1 to 1,300 and 250 to 1,500 respectively. Those results may be represented analytically by the equation :

$$C = \lambda\, (Re_d)^{0.088} \qquad (3)$$

On averaging, by a least square fit for each fluid, the value of the type of loss coefficient λ was found to vary between 0.62 and 0.97 (Table 1). Thus the equation (3) represents C vs. Re_d with less than 10 % dispersion. The graph representing C vs. Re_c for rising bubbles [4] it also shown for comparison. The main difference is again that the C-curve does not show a minimum in the case of rising drops.

The rising drops photographed show a spherical shape when $D < 0.3$ cm, and an oblated spheroidal one, on their superior part, when $D > 0.6$ cm. Falling drops assume similar forms [6, 7, 15], for other ranges of diameters however. The direction of motion has thus little influence on the shapes of the drops.

The use of two cameras focusing in perpendicular planes leads to one of the main results of the present work. Previous research generally carries the implicit assumption that the manner of fall or rise of deformable particles is a fixed property of the system. The path had been found to be [3, 6, 7, 16, 20] straight, irregular or circular helicoidal and straight again, for small, medium and large particles respectively. In a preceeding paper however [20], it was shown that the type of drop fall depends on the mode of release.

In this work it is shown that even after having reached constant velocity component U, the trajectory of drops follows a path approximately given by an elliptical spiral and a damped sinusoid in horizontal and vertical projection

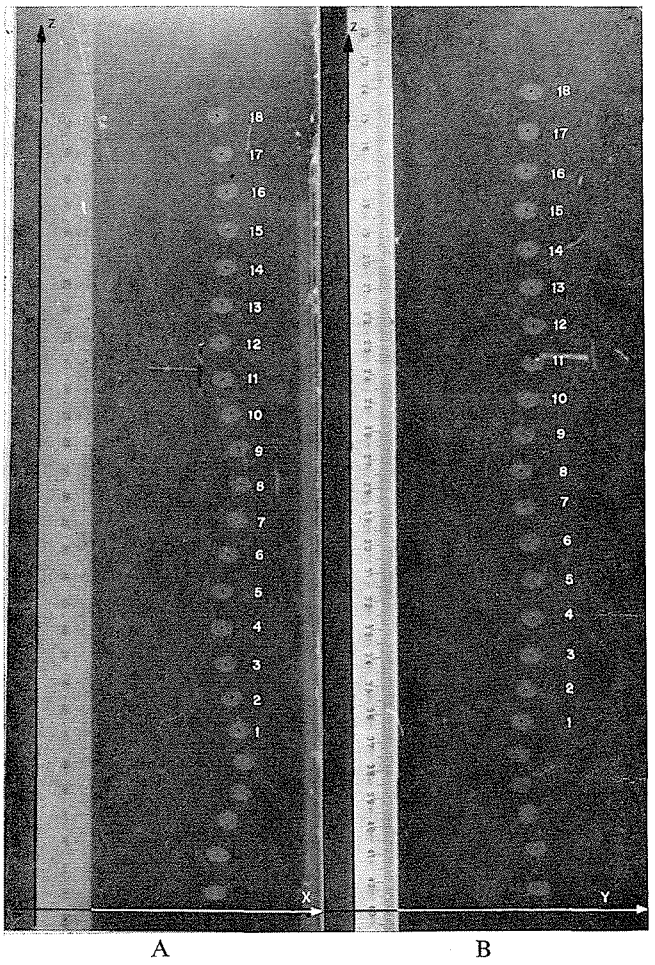

4/ Plate A and B, showing rise of the same xylene drop, taken simultaneously from camera A and B respectively, focusing in perpendicular planes.

Photographies A et B qui montrent l'ascension de la même goutte de xylène et qui furent prises simultanément par les caméras A et B respectivement dans des plans perpendiculaires.

respectively. This is shown on Figure 5 by constructing, from Plate A and B of Figure 4 (taken simultaneously from camera A and B respectively - see Fig 1), a typical path made by a xylene drop of D = 0.75 cm rising with constant velocity component U = 13.0 cm/s. The 30 cm of rise —made with constant velocity component U—photographed, shows an exponential type of damping of the oscillations drifting towards vertical rise. The 4 pairs of plates, taken for each one of the 6 discontinuous phases and 14 drop's volume, show a variation in the dimensions of the exponential helix described above. Thus the path (before being vertical) of drops rising with constant velocity component U, is not a fixed property of the system only, but also depends on initial conditions. It was not possible to find out which elements, in the slow process of formation and release used, could determine the parameters of the equations :

$$\begin{aligned} \overline{X} &= A\, e^{-\alpha t} \cos \omega t + \overline{A} \\ \overline{Y} &= B\, c^{-\alpha t} \sin \omega t + \overline{B} \\ Z &= Ut \end{aligned} \qquad (4)$$

describing approximately the trajectory photographed. It was nevertheless observed (Fig. 5) that the slope of the path is of order 6, for the first period of pseudo oscillation made with constant U. The variation of the slope of the velocity vector (from about 6 to ∞) is noteworthy considering its constant vertical component. The ratios A/D et B/D, most encountered in the 6 × 14 experiments carried out, were approximately 1.0 and 0.1 respectively. The damping characteristic of the amplitude of the oscillation α varies greatly about and average value of 0.87 with a maximum of 2.

The helicoidal type of motion observed suggests that a spin is given to the drops at the moment of detachment, due to some hardly noticeable particularities of the releasing process. Thus, in the case of clockwise helicoidal rise (Fig. 5), a counter-clockwise spin would explain the centripetal force associated with that motion. This spin would gradually disappear, due to friction, and thus the path would tend towards the vertical. At that time only could the drops be said to be in steady regime. As no reliable information could be gathered about the internal motion, the influence of the kinematic viscosity could not be evaluated.

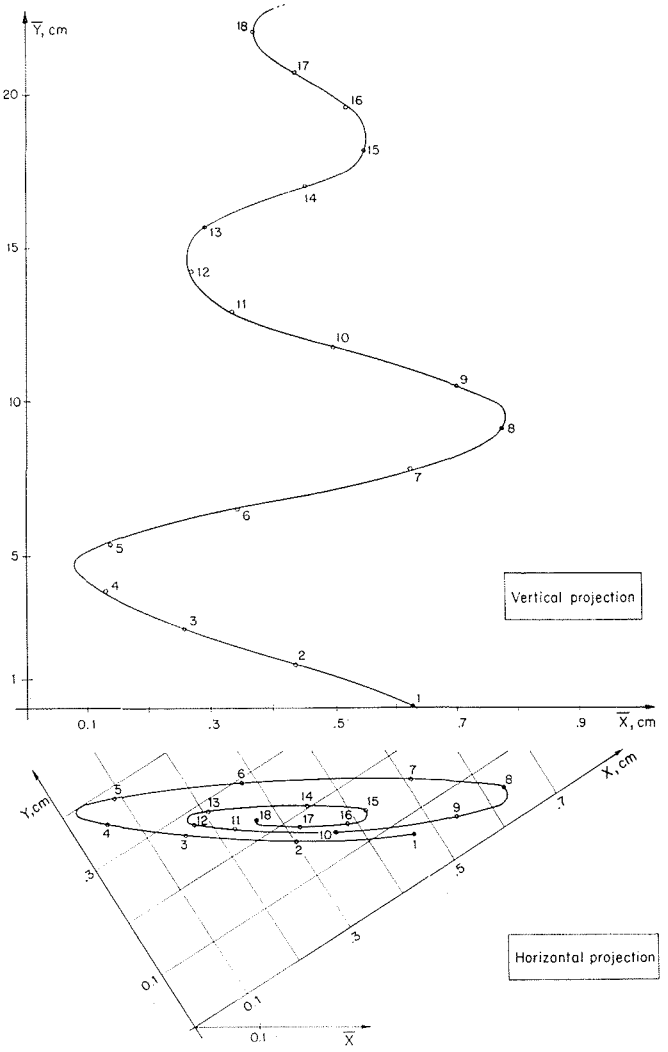

5/ Construction of path of a xylene drop of D = 0.75 cm rising with U = 13.0 cm/sec, based on plates A and B of figure 4.

Reconstitution du parcours d'une goutte de xylène (D = 0,75; vitesse de montée U = 13,0 cm/s) à l'aide des photographies A et B de la figure 4.

Acknowledgment

The authors acknowledge the helpful suggestions of Professors H. Cabannes, J. Fremau and A. Rocha and the valuable assistance of Messrs. H. Franceschi and E. Horcades in the photographic work.

Notation

Subscripts $_c$ and $_d$ refer to continuous and discontinuous phases respectively.

C	: drag coefficient
D	: diameter of equivalent sphere, cm;
F_r	: Froude's Number, $U/\sqrt{(gD)}$;
g	: gravitational acceleration, cm/s^2;
Re_c and Re_d	: Reynolds numbers, $DU\rho_c/\mu_c$ and $DU\rho_d/\mu_d$ respectively;
U	: constant vertical velocity component, cm/s;
λ	: adimensional discontinuous phase' constant;
μ	: viscosity, cP;
ρ	: density, g/cm^3.

References

[1] ARIS (R.). — *Vectors, Tensors and the Basic Equations of Fluid Mechanics.* Prentice-Hall, 1962.

[2] BATCHELOR (G. K.). — *An Introduction to Fluid Dynamics.* Cambridge University Press, 1967.

[3] SAFFMAN (P. G.). — *J. Fluid Mech.*, 1956, *1*, 249.

[4] HABERMAN (W. L.) and MORTON (R. K.). — *Trans. Am. Soc. Civil Engrs.*, 1956, *121*, 227.

[5] DAVENPORT (W. G.), RICHARDSON (F. D.) and BRADSHAW (A. V.). — *Chem. Engng. Sci.*, 1967, *22*, 1221.

[6] SATAPATHY (R.) and SMITH (W.). — *J. Fluid Mech.*, 1961, *10*, 561.

[7] WINNIKOW (S.) and CHAO (B. T.). — *Physics Fluids*, 1966, *9*, 50.

[8] LEVICH (V. G.). — *Physicochemical Hydrodynamics.* Prentice-Hall, 1962.

[9] CHAO (B. T.). — *Physics Fluids*, 1962, *5*, 69.

[10] MOORE (D. W.). — *J. Fluid Mech.*, 1963, *16*, 161.

[11] COLLINS (R.). — *J. Fluid Mech.*, 1966, *25*, 469.

[12] LUIZ (A. M.). — *Chem. Engng. Sci.*, 1967, *22*, 1083.

[13] THORSEN (G.), STORDALEN (R. M.) and TERJESEN (S. G.). — *Chem. Engng Sci.*, 1968, *23*, 413.

[14] HARPER (J. F.) and MOORE (D. W.). — *J. Fluid Mech.*, 1968, *22*, 1083.

[15] TAYLOR (T. D.) and ANDREAS ACRIVOS. — *Chem. Engng Sci.*, 1964, *19*, 471.

[16] UNO (S.) and KINTNER (R. C.). — *J. Am. Instn. Chem. Engrs.*, 1956, *2*, 420.

[17] GARNER (F. R.) and LANE (J. J.). — *Trans. Instn. Chem. Engrs.*, 1959, *37*, 162.

[18] LANE (W. R.) and GREEN (H. L.). — *Surveys in Mechanics.* Cambridge University Press, 1956.

[19] BIRKHOFF (G.). — *Hydrodynamics.* Princeton University Press, 1950.

[20] MERCIER (J.) and ROCHA (A.). — *Chem. Engng Sci.*, 1969, *24*, 1179.

[21] LAMB (H.). — *Hydrodynamics.* 6th Edn, Cambridge University Press, reprinted by Dover Publications, 1945.

[22] ROSENBERG (B.). — *Report n° 727, David Taylor Model Basin.* U.S. Dept. of the Navy, Washington, D.C., 1950.